



Developing polyimide-copper antifouling coatings with capsule structures for sustainable release of copper



Yi Liu, Xinkun Suo, Zhe Wang, Yongfeng Gong, Xin Wang, Hua Li*

Key Laboratory of Marine Materials and Related Technologies, Zhejiang Key Laboratory of Marine Materials and Protective Technologies, Ningbo Institute of Materials Technology and Engineering, Chinese Academy of Sciences, Ningbo 315201, China

ARTICLE INFO

Keywords:

Polyimide
Copper biocides
Antifouling
Liquid flame spray
Capsule structure

ABSTRACT

Polyimide-copper layers consisting of individual capsule-like splats were one-step fabricated by solution precursor flame spray through controlling the reaction between dianhydride and diamine dissolved in copper nanoparticles-containing dimethylformamide solvent. The polyimide splat exhibited hollow structure with an inner pore of 10–15 μm and a tiny hole of 1–5 μm on its top surface. Transversal cut by focused ion beam milling of the individual splats and scanning electron microscopy characterization further revealed unique dispersion of the copper nanoparticles inside the polyimide shell. After 1000 h exposure to the testing synthetic seawater, continuous release of copper from the coatings containing up to 30 wt%Cu kept remarkable. Antifouling performances of the constructed layers were assessed by examining colonization behaviors of typical bacteria *Bacillus* sp. and marine algae *Phaeodactylum tricornutum* and *Chlorella* on their surfaces. Distribution of the inorganic nanoparticles endows the polyimide coatings with special capsule structure and exciting hydrophobicity and antifouling performances. The liquid flame spray route and the encapsulated structure of the polyimide-Cu coatings would open a new window for designing and constructing environment-friendly marine antifouling layers for long-term applications.

1. Introduction

Any surface immersed in seawater is prone to the settlement of marine organisms, such as protein, bacteria, algae, or mollusks [1]. As a consequence, artificial marine infrastructures usually suffer from biofouling attacks throughout their services in the marine environment [2,3]. Among the measures taken so far to solve the abovementioned problems, construction of an antifouling layer has been proven to be effective in offering long-term antifouling performances. However, due to complexity of the marine environment and diversity of the fouling species, universality and sustainability still remain as the two main challenges for man-made antifouling coatings. The antifouling technique based on the use of biocides has been the most widespread approach in modern maritime industries [4]. During the last decades, however, growing awareness of environmental issues pertaining to the use of biocides have triggered booming research efforts in searching green alternatives [5]. There is also a growing demand for surface protection techniques that meet the requirements of material durability and environmental sustainability.

Exciting research progresses have been made in recent years towards developing novel environment-friendly antifouling materials

and coatings, some of which have shown promising performances, for example nontoxic or green biocides [6–8], new organic matrixes [9,10], new embedding [11,12] and encapsulating technologies [13,14], photo-induced nanocomposites [15], and the antifouling structures mimicking natural hydrophobic surfaces [16]. Copper has been the most important alternative biocide since organotin compounds were banned. Various copper agents including copper metal, copper alloys, copper oxides, and copper compounds have been used as principal biocides for decades [17–20]. Regardless of the role copper plays as the essential element for marine organisms, it is still a big concern about its tolerable concentration, above which unexpected deterioration usually happens to marine species. Design and fabrication of smart coatings with appropriate structure for sustainable release of copper ions for long-term antifouling performances are therefore essentially required.

It is established that for biocides-involved antifouling techniques, effective prevention of fouling is usually achieved by controlled release of the biocides from matrix materials. Copper nanowire films and their incorporation into elastomeric polydimethylsiloxane exhibited the low levels of copper ions released after 50 days [19]. In addition, it was reported that chemically bound acrylated copper nanoparticles showed significantly reduced amount of copper ions leaching from functiona-

* Corresponding author.

E-mail address: lihua@nimte.ac.cn (H. Li).

lized Cu nanoparticles compared to nonfunctionalized biocides [20]. The major hurdle for widespread use of copper ions for antifouling applications is yet how to effectively control their release. Long-term sustainable release of the biocides is crucially influenced by matrix materials and physicochemical interaction of biocides with the matrix. For application in the marine environment, it is essential that matrix materials are stable in terms of anti-corrosion/wear in seawater, apart from the ease of making the biocides-containing structure.

To achieve constrained release of copper ions without deteriorating antifouling efficiency, the measures taken to incorporate copper into polymeric matrices are to be further explored. Due to their inert nature, polymers as surface coatings on metal surface could act as barrier resisting invasion of corrosive species and fouling organisms [21]. Among the polymeric materials developed for marine applications, aromatic polyimide attracted extensive attention owing to its excellent mechanical properties, superior thermal stability, good chemical resistance and processability [22,23]. To date, cross-linking is the most commonly used approach for fabrication of polyimide coatings [22]. As an alternative processing route, thermal spray in particular flame spray was proven successful in fabricating polymer coatings for its advantages of easy operation, cost efficiency, and capability of large-scale manufacturing [24,25]. However, fabrication by thermal spray of polymer-based composite coatings keeps challenging for spraying the polymers in the form of powder, due mainly to the difficulties in incorporating the additives like copper particles into polymeric matrix. Liquid flame spray that employs liquid as the starting feedstock for coating deposition has the potential for one-step fabrication of polymer-encapsulated composite coatings. Desired additives can be easily added into the liquid for subsequent deposition of the coatings with unique dispersion of the second phases. It is anticipated that liquid thermal spray approach provides controllable heat input for synthesis of polyimide during the spraying. To date, however, there are few reports available pertaining to thermal sprayed polyimide-based coatings, deposition mechanism of hollow capsules and related knowledge of polyimide coatings for marine antifouling applications is still lacking.

In this paper, liquid flame spray route was proposed for constructing copper-containing polymer coatings. Nano copper particles were added in polyimide precursor for subsequent synthesis of polyimide and coating fabrication. Microstructural features of individual polyimide-copper splats and coatings were characterized by focused ion beam technique and antifouling performances of the coatings were assessed by examining colonization behaviors of *Bacillus* sp. and *Phaeodactylum tricornutum* and *Chlorella*. This research provides a new processing route for large-scale fabrication of capsules with polymer as shell and inorganic particles as filler.

2. Materials and methods

2.1. Synthesis of polyimide and polyimide-Cu precursors

Kapton-type aromatic polyimide precursor solution was prepared by mixing monomer pyromellitic dianhydride (PMDA, 80,112,127 CP, Sinopharm Chemical Reagent Co. Ltd., China) and 4,4'-oxydianiline (ODA, 30049926CP, Sinopharm Chemical Reagent Co. Ltd., China) in dimethylformamide (DMF) solvent. For the polyimide-Cu suspension preparation, Cu particles with the size of ~300 nm were dispersed in DMF-ODA at room temperature with the stirring speed of 200 r/min for 5 h. Then PMDA was added into the above solution with an equivalent molar ratio to ODA. The polycondensation occurred at room temperature for 12 h and Poly (amic acid) (PAA) -Cu precursor solution was obtained. PAA-Cu solutions with different contents of Cu (0, 10 wt%, 20 wt%, and 30 wt%) were prepared. The synthesis of polyimide during flame spray was based on the chemical reaction shown in Fig. 1a.

2.2. Fabrication of coatings

The liquid precursor solution was atomized and injected into the oxygen-acetylene flame where the liquid phase was evaporated and thermochemical reactions were completed to produce coatings. The coating fabrication by the liquid flame spray is schematically depicted (Fig. 1b). During the spraying, the precursor suspensions were atomized by a home-made spray atomizer. The precursor feedstock injector with a diameter of 1.5 mm was positioned just next to the flame torch, and the angle between the injector and flame was 30°. Pressure of the atomizing air was 0.7 MPa. Prior to coating deposition, the grit-blasted carbon steel Q235 plates and polished stainless steel substrates were rinsed in distilled water and ultrasonically cleaned in acetone. The spraying was carried out using the Castodyn DS 8000 system (Castolin Eutectic, Germany). For the liquid flame spraying, acetylene was used as the fuel gas with the flow rate of 1.5 Nm³/h and working pressure of 0.1 MPa. Pressure and flow rate of oxygen were 0.5 MPa and 2.5 Nm³/h respectively. The precursor feed rate was 40 ml/min and the spray distance was 200 mm.

2.3. Characterization of microstructure

Microstructure of the splats and the coatings was characterized by field emission scanning electron microscopy (FESEM, S4800, Hitachi, Japan). For further examination, focused ion beam (FIB) milling of the samples was performed in a FIB/scanning electron microscope dual beam system (Helios Nanolab 660, FEI, USA). Transversal cut of the samples was carried out at a stage tilt of 52°. A focused beam of Ga⁺ ions was rastered across the specimen surface. Larger beam currents quickly milled away sections of material from the sample surface, while lower currents were used for polishing the milled surface. The samples were also analyzed by fourier transform infrared spectroscopy (FTIR, Nicolet 6700, Thermo Fisher Scientific, USA) with the resolution of 4 cm⁻¹ and a scan range of 4000–400 cm⁻¹. Release rate of copper ions from the coatings as a function of immersion time was also examined through measuring the concentration of copper ions in testing solution using inductively coupled plasma mass spectrometer (ICP-MS, NexION 300, USA). For the measurement, the coating samples were exposed with an area of 2 × 2 cm in artificial seawater (ASW) prepared according to the ASTM D1141–98 (2003). Wettability of the coating samples was assessed by measuring the contact angle of deionized distilled water droplets spreading on their surfaces using a contact angle measurement instrument (Dataphysics OCA20, Germany).

2.4. Antifouling testing

Antifouling performances of the coatings were assessed by examining formation of bacterial biofilm and colonization of algae on their surfaces. Marine *Bacillus* sp. (MCCC No. 1A00791) was used in this study. *Bacillus* sp. bacteria were cultured in 2216E (CM 0471) media prepared by dissolving 1 g yeast extract, 5 g peptone, 1 g beef extract, and 0.01 g FePO₄ in 1000 ml deionized water. The media containing the bacterial strains were shaken for 24 h at 25 °C. The inoculated medium was prepared by adding *Bacillus* sp. for an initial concentration of 10⁶ CFU/ml at 25 °C under aerobic conditions. For FESEM observation of the bacteria attaching on the surfaces of the samples, the bacteria after 48 h incubation were fixed in 2.5% glutaraldehyde for 24 h, dehydrated gradually and coated with gold. Diatoms *Phaeodactylum tricornutum* (provided by Ningbo University, China) and green algae *Chlorella* sp. (provided by Ningbo University, China) were used in this study to further clarify the antifouling performances of the coatings. The microorganisms were cultured in artificial seawater-based culture media under sterile conditions at 20 °C. Adhesion of the algae on the surfaces of the samples for 1 week was inspected. After the fixation by 2.5% glutaraldehyde for 1 h, the samples were

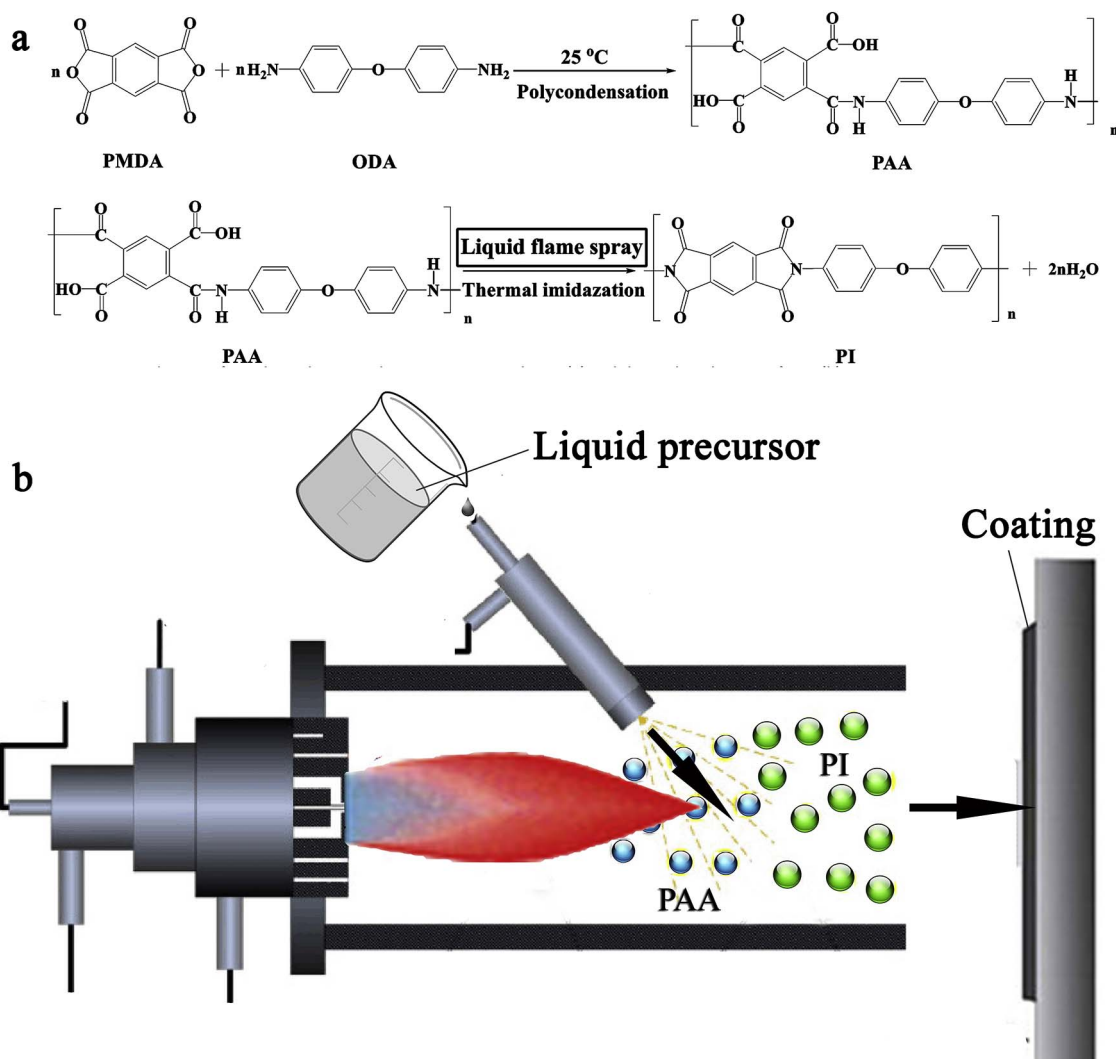


Fig. 1. The synthesis route for polyimide during the liquid flame spray (a), and schematic representation of the spraying (b).

observed by confocal laser scanning microscopy (CLSM, TCS SP5, Leica, Germany).

2.5. Electrochemical testing

For the corrosion testing of the coatings, potentiodynamic polarization and electrochemical impedance spectroscopy (EIS) spectra were acquired on Solartron Modulab system (2100A, UK). All the testing was conducted at room temperature in ASW. Prior to the impedance testing, the working electrode was maintained in the testing environment for 30 min. At least three specimens were tested for each sample and each set of experiments was repeated three times to ensure reproducibility. A traditional three-electrode cell was used, with 1 cm² platinum as the counter electrode, a saturated calomel electrode as the reference electrode and the specimen with an exposure area of 1 cm² as the working electrode. Potentiodynamic polarization curves were acquired with a potential range from –1300 mV to 700 mV versus E_{ocp} at a scan rate of 0.5 mVs⁻¹. EIS measurement was performed with an applied ac signal of 10 mV and the frequency ranging from 100 kHz to 0.01 Hz. After the measurement, the acquired data were fitted and analyzed using a ZSimpWin software based on equivalent circuit models. The corrosion rate (R_{corr} , in millimeter per year) was calculated from the following equation [26]:

$$R_{corr} (\text{mm/year}) = \frac{[I_{corr} (\text{A/cm}^2) \cdot M (\text{g})]}{D (\text{g/cm}^2) \cdot V} \times 3270,$$

where I is current (A/cm²), M is molecular weight, V is valence, and D is the density (g/cm³).

3. Results and discussion

Polyimide and nano copper-containing polyimide coatings were successfully fabricated by the liquid flame spray deposition. Cross-sectional view of the coatings shows typical lamellar morphological feature of thermal sprayed coatings and porous microstructure (Fig. 2a). Our previous finding implies that micron-sized copper unlikely gives rise to capsule structure [27]. Surprisingly, it is noted that the nano copper-containing polyimide coatings exhibit a typical capsule structure with copper nanoparticles being enwrapped by polyimide (Fig. 2b). The coating comprises individual micro-capsules and close interconnection among them is seen (Fig. 2a), leaving no obvious through-thickness flaws. This feature offers the probability of release of the encapsulated antifoulants in a controllable manner. The microcapsules are small particles with biocides as core materials being surrounded by polymer shell. It is anticipated that this structure might also give rise to long-term survival of the coatings against biofouling in harsh marine environment. Enlarged inner views of the coatings clearly show dispersed single Cu particles and agglomerated Cu clusters that are encapsulated by polyimide layer (Fig. 2c and d). Micro-capsules are

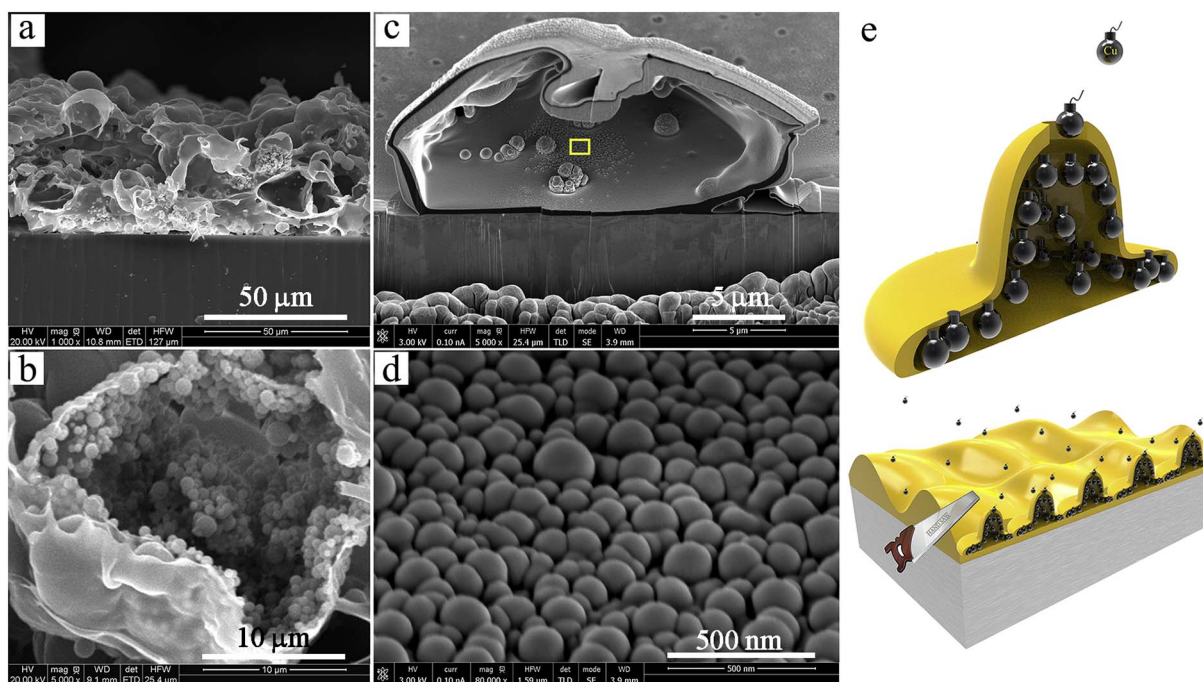


Fig. 2. Microstructure of the polyimide-30 wt%Cu coatings and splats, a: cross-sectional SEM view of the polyimide-copper coating, b: enlarged view of one fractured polyimide-Cu splat, c: FIB dissection of the polyimide-Cu splat, d: enlarged view of the selected area in c showing agglomerated Cu nanoparticles, and e: schematic depiction of the polyimide-Cu coatings with capsule structure.

uniformly distributed in the coatings and copper nanoparticles exhibit an entrapped state, in turn avoiding undesirable interaction between active Cu and seawater for spontaneous leakage. This is exciting since polyimide is physicochemically stable and performs well in seawater. The polymeric shell controls diffusive release of the biocide to the surrounding medium for marine antifouling (Fig. 2e) while protecting the remaining encapsulated biocide from possible corrosion.

It is well established that thermal sprayed coatings are built up by the accumulation of individual splats, which usually involves impingement of molten/partially molten particles and subsequent quenching. The particle parameters such as velocity, temperature, and degree of solidification, and substrate variables affect the flattening behaviors [28]. PAA and PAA-Cu precursor solutions were initially synthesized via in situ polymerization and following thermal imidization by flame spraying. During the spraying, combustion products of DMF solvent are carbon oxides (CO, CO₂), nitrogen oxides (NO, NO₂), etc. Consequently, high temperature heating results in solvent evaporation and water loss in PAA macromolecules [29], leading to generation of gas in particle core. This presumably accounts mainly for the microsized hollow polyimide spheres formed in the coatings. The quenching-induced solidification of polyimide obviously results in constrained escape of the gas generated during imine formation.

To further elucidate the formation mechanisms of the structure, polyimide particles were collected by spraying the precursor directly into distilled water contained in a stainless steel container and further dried. Spherical polyimide particles with perfect capsule structure are attained (Fig. 3a) and they have the sizes consistent to the spheres shown in the coatings. It is noted that the spheres have smooth surfaces and no open holes are seen. Further characterization of individual polyimide splats collected on stainless steel substrate suggests their well-flattened morphology (Fig. 3b) and trace of gas escape during flattening stage (Fig. 3c). These phenomena are schematically depicted in Fig. 3d. Accumulation formation of thermal sprayed coating on fresh substrate surface is a complex dynamic process. For hollow droplet like polyimide droplet in this case, upon its impact on substrate, liquid jets out from the bottom of the droplet and spreads in the radial direction (jetting-out region B in Fig. 3d), but solidification is usually fast enough

so that solidification of the portion of the droplet in contact with substrate would have completed (bonded region A in Fig. 3d). High-velocity impact would result in sudden increase in inner pressure of the hollow sphere, in turn likely triggering breaking along the direction opposite to the impact to form a tiny hole (top hole zone C in Fig. 3d).

The structural features of the flattened polyimide-based particles were further examined by SEM through milling the splats with Ga⁺ beam by FIB. Prior to dissection of the splats, a protective strip of platinum was deposited (inset in Fig. 4a) over the site of interest (Fig. 4a) and appeared as a lighter layer covering the sectioned splat (Fig. 4b and c). The cross-section of the hat-like polyimide splat clearly shows the hollow structure (Fig. 4b and c). The thickness of the thin bottom layer, the lateral, and the upper shell varies showing the value of ~0.2 μm, ~1.5 μm, and ~4 μm, respectively. The inner surfaces of the hollow splat are smooth and it is interesting to note that the polyimide splat bonds very well with the substrate and the intimately contacting polyimide layer has the thickness of 0.1–0.3 μm (Fig. 4b and c). This is important since the well-bonded polyimide-substrate interface provides the coatings with favorable adhesive strength. It should be noted that prior to the deposition, the substrate was already pre-heated by the flame spray gun. Surface pre-heating causes removal of absorbed gas and formation of Fe₂O₃ layer on the surface, which probably increases the contact resistance and further promotes spreading of impinged droplets [28]. To gain further information about the exceptional structure, subsequently impacted droplet on the pre-flattened splat was also characterized by FIB approach (Fig. 4d). Excellent cross-linking is recognized between the adjacent two splats (Fig. 4d and e). Interestingly, sectioned view shows unnoticeable interface in between the splats at their bottom layers (Fig. 4f). It should be noted that the splats have isolated inner pores of ~12 μm and top holes of 1–5 μm. This special capsule structure is promising for controlled release of packed biocides for potential antifouling functions. In addition, the flawed morphology at the center of the top layer of the splat (Fig. 4a and d) further proves our speculation (as depicted in Fig. 3d) that the possible gas leakage as a result of sudden increase in inner pressure of the hollow sphere easily results in formation of the through hole.

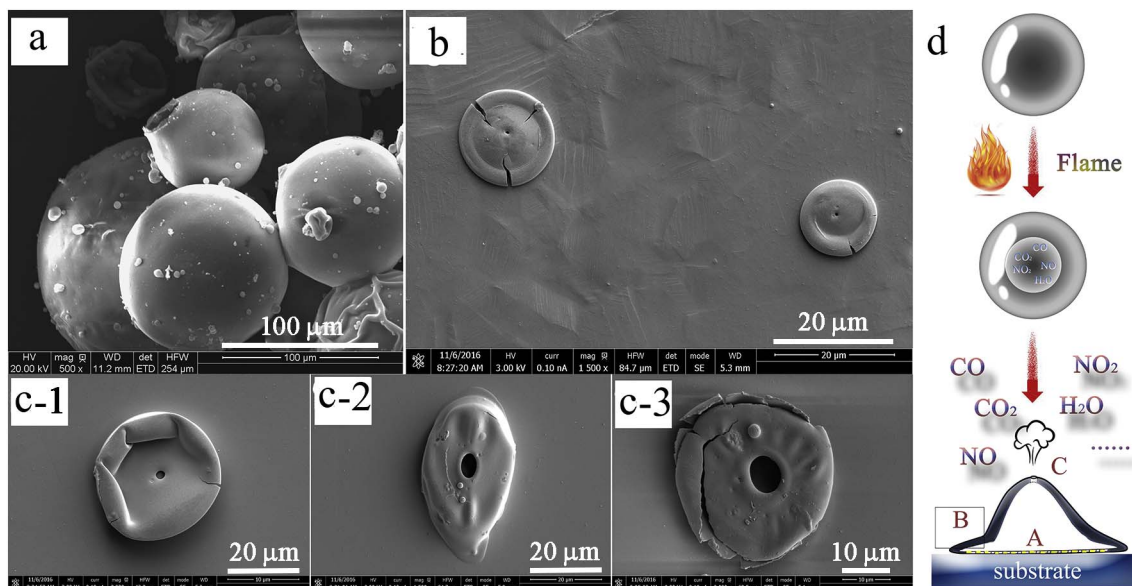


Fig. 3. Morphology of the as-sprayed powder and splats, a: polyimide hollow spheres, b: polyimide splat deposited on stainless steel preheated at 350 °C, c: polyimide splats deposited on stainless steel preheated at 150 °C (c-1, c-2, and c-3 show three typical splats with different sizes of the top hole), and d: schematic diagram showing formation regime of the top hole (A: bonded zone, B: jetted-out zone, and C: top hole zone).

Thermal spray technique already showed great potential for synthesis of new materials [30,31]. It seems clear that flame spray has accomplished complete synthesis of polyimide by thermal imidization during the coating deposition. Degree of imidization was examined by FTIR (Fig. 5a). IR spectra of the polyimide coatings display the characteristic peaks at 1720 cm^{-1} for symmetric stretching vibration of C=O, 1780 cm^{-1} for asymmetric stretching vibration of C=O, 1380 cm^{-1} for CN stretching vibrations, and 725 cm^{-1} for bending vibration of C=O. For all the as-deposited coatings, full imidization has been achieved. This is not surprising since liquid droplets of polyimide precursor solution injected into the flame are subject to a relative controllable temperature range which is suitable for thermal imidization [24].

Further electrochemical testing was carried out for the coatings, since corrosion resistance is one of the essential requirements for the

coatings for marine applications. Results show that E_{oc} of the polyimide and polyimide-Cu coatings in artificial seawater is more positive and corrosion current density is obviously lower than that of carbon steel Q235 (Fig. 5b). Electrochemical impedance spectroscopy (EIS) is a powerful non-destructive approach for characterizing electrochemical reactions at coating/ASW interfaces. It is realized that the impedance acquired from Nyquist plots of the coatings immersed in ASW is higher than the uncoated Q235 immersed in ASW (Fig. 5c), indicating better anti-corrosion performances of the coatings. Assessment of corrosion rate (R_{corr} , in millimeter per year) of the coatings showed the R_{corr} value of 2.6×10^{-2} mm/year, 4.1×10^{-4} mm/year, 2.5×10^{-4} mm/year, 3.2×10^{-3} mm/year, and 2.1×10^{-3} mm/year for the uncoated Q235, the pure polyimide coating, the polyimide-10 wt%Cu coating, the polyimide-20 wt%Cu coating and the polyimide-30 wt%Cu coating, respectively. This nevertheless suggests that the polyimide coating

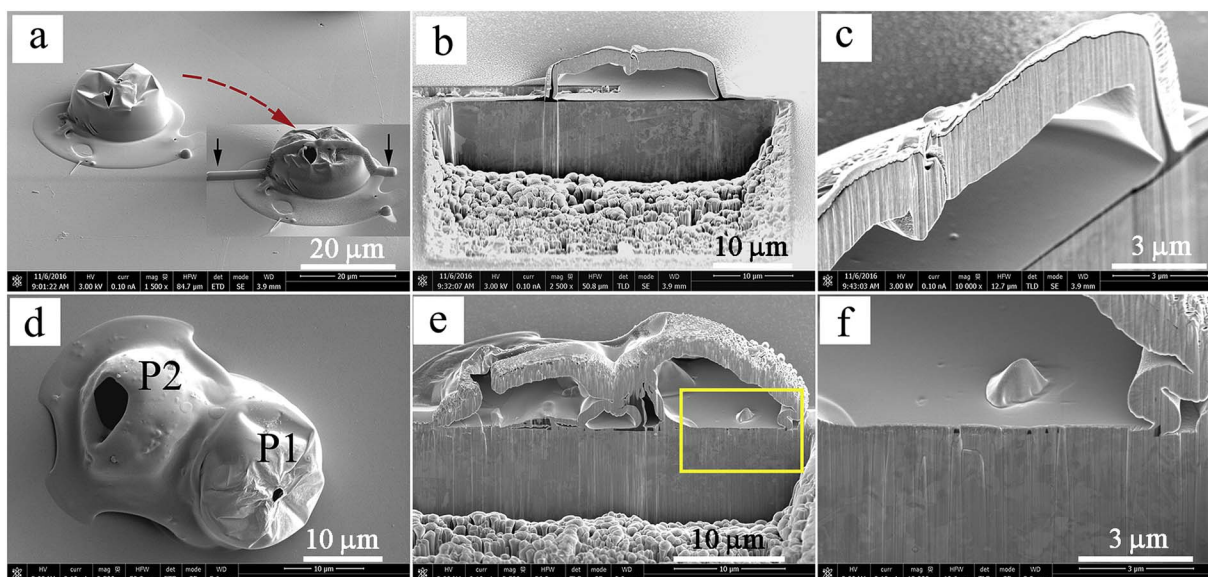


Fig. 4. Morphologies of the as-deposited polyimide splats as revealed by FESEM characterization after FIB dissection, a: single splat before milling (the inset in a shows deposition of Pt strip over the site of interest for the transversal cut), b: cross-sectional view of the polyimide splat shown in a, c: enlarged view of selected area of b; d: twin polyimide splats showing complete cross-linking between the laterally impacted adjacent splats (P1 and P2), e: cross-sectional view of the splats showing the twin-hollow structure, and f: enlarged view of the selected area in e.

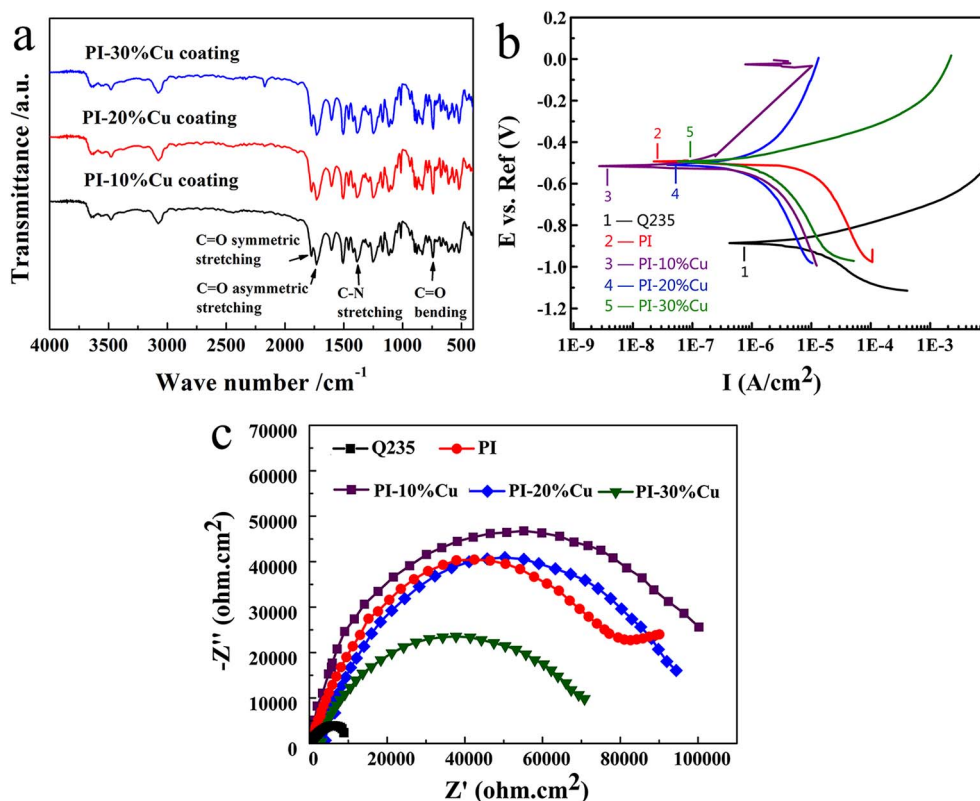


Fig. 5. Characteristics of the coatings and their electrochemical performances, a: FTIR spectra of the coatings, b: potentiodynamic polarization curves, and c: Nyquist plots of the coatings tested in ASW.

alone already significantly enhanced the anti-corrosion properties of the steel substrate, which is likely attributed to the special capsule structure and the well-bonded interconnecting state of adjacent capsules.

It is known that the effectiveness of biocides differs depending on their concentration (release rate) and exposure duration. Therefore, controlling the release from the capsules is of top importance [32]. Morphologies of the polyimide splats already showed exciting hollow structures and copper nanoparticles are distributed inner polyimide shell. The tiny top hole of the polyimide splat would facilitate sustained release of copper ions. Further assessment of the releasing of copper ions shows that the polyimide-Cu coatings immersed in ASW for 48 h exhibit the formation of many flower-like particles on their surfaces (Fig. 6a). The individual particles have nearly spherical shape with an average size of $\sim 3 \mu\text{m}$. This structure is similar to a previously reported 3D nanostructure of CuO micro balls obtained by hydrothermal methods [33]. Release rate testing of copper from the coatings suggests

continuous yet relatively stable release (Fig. 6b). It is not surprising that higher content of copper in the coatings brings about higher release rate. Compared to the biocide-encapsulated coating, mixture of polyimide and Cu powder without encapsulated structure shows 11 times faster release rate. Polyimide as the shell in the coatings protects efficiently quick consumption of copper by the seawater, which is promising for long-term antifouling functions.

In addition, antifouling properties of the Cu-free and the Cu-containing polyimide coatings against marine bacteria were examined. For marine applications, surface characteristics in particular wettability and surface energy of the layers play important roles in deciding their biocide-release, antifouling, and anti-corrosion performances. It is clear that the addition of Cu particles altered the surface wettability of the coatings (the inset in Fig. 7a). The coatings turn to be hydrophobic after addition of Cu particles and increase in Cu content brought about significantly increased water contact angles. The angle increases from $\sim 68^\circ$ for the pure polyimide coating to $\sim 131^\circ$ for the layer comprising

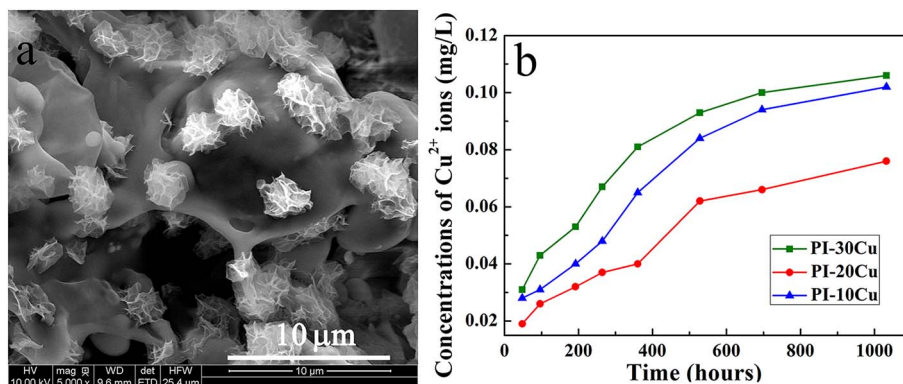


Fig. 6. Release features of Cu nanoparticles from the PI-Cu coatings. a: topographical view of the polyimide-Cu coating after being incubated in seawater for 48 h, and b: concentration of copper in the testing solution versus incubation duration.

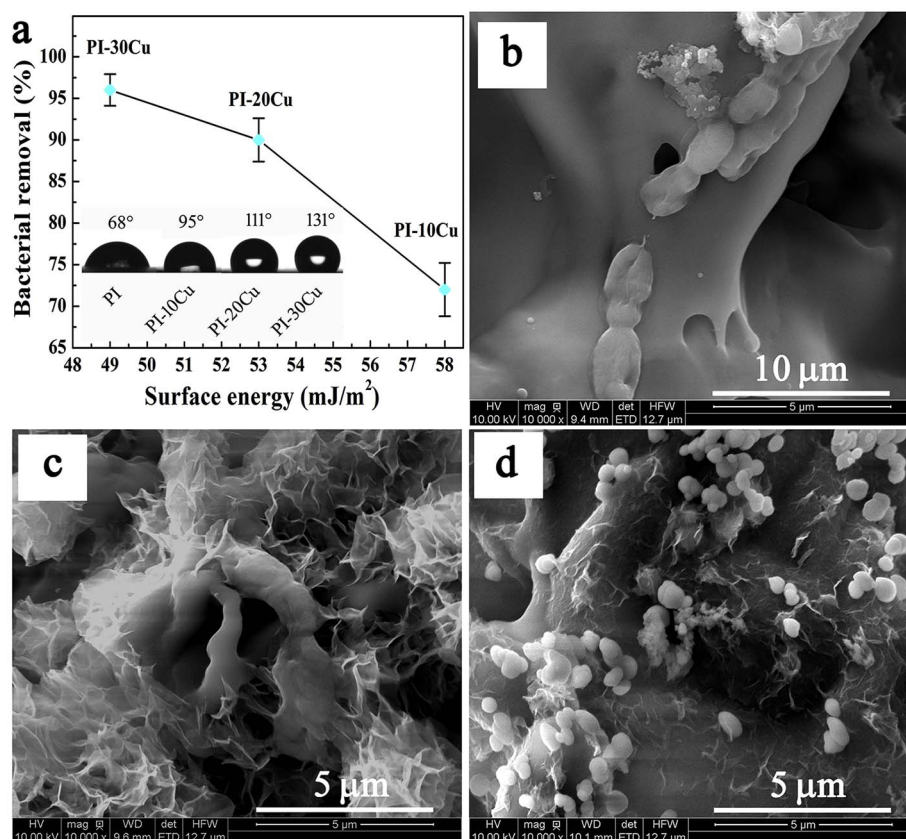


Fig. 7. Quantitative analyses of the adhered bacteria on the coatings, a: bacterial removal ratio versus surface energy of the polyimide-Cu coatings (the inset is the optical photos of the water droplets standing on the surfaces of the coatings); b, c, d: SEM images showing the morphology of the adhered *Bacillus* sp. bacteria on the polyimide-10 wt%Cu coating (b), the polyimide-20 wt%Cu coating (c), and the polyimide-30 wt%Cu coating (d).

30 wt%Cu. Hydrophobicity is generally explained as a result of reduced surface energy due to the combination of micro-hollow polyimide capsule and Cu nano-particles [34,35]. Besides, this hierarchically micro-nano-structured capsules give rise to air-trapping below the droplet on the coating surface, forming Cassie's state [34]. This hydrophobicity likely promotes anti-corrosion performances of the coatings and constrains release of copper from the coatings. In fact, design of antifouling structure based on hydrophobic surface [16,36] and encapsulated biocides [13,14] is a promising method towards preventing biofouling in modern maritime industries.

Excellent sterilization performances were further revealed for the Cu-containing coatings (Fig. 7a). For the coatings containing 20 wt%Cu and 30 wt%Cu, disappearance of the bacterial colonies in the *Petri* dishes indicates that most of the bacteria were killed by copper ions. After 12 h exposure, ~100% bacteria were already extinguished (data not shown). Further examination of bacterial adhesion shows that after being immersed in the bacteria-containing seawater for 2 days, the percentage of bacterial removal strongly correlated with the surface energy of the coatings. The removal percentage decreases with increasing surface energy of the coatings (Fig. 7a). The Cu-containing polyimide coatings exhibit remarkable bacterial removal and increased Cu content in the coatings gives rise to enhanced removal (Fig. 7b, c, and d). For the polyimide-30 wt%Cu coating, there are a large number of spores instead of bacteria seen on its surface (Fig. 7d). Copper typically exists as Cu (II) outside bacterial cell and Cu (I) inside the cell. It was evidenced that binding of heavy metals to the DNA of bacteria and bacterial spores occurred [37]. The DNA in dormant spores of *Bacillus subtilis* as well as other *Bacillus* species is extremely well protected against damage resulting from treatments such as desiccation, heat, oxidizing agents, or UV and γ radiation. This high degree of DNA protection is a major factor for species survival when subjected to

environmental stresses [38]. Moreover, it is observed that the biocides release is promoted against *Bacillus* sp., and obvious CuO layer is seen on the surface area (Fig. 7c and d), possibly indicating more adhered bacteria, which in turn facilitates secreted extracellular polymeric substances (EPS) and biofilm-triggered corrosion of Cu [39].

To gain further insight into antifouling performances of the coatings with the capsule structure, adhesion of typical algae on the polyimide-based layers were examined. After 1 week of exposure, algae no uniformly adhered on the areas where the capsules are seen on the surface of the polyimide-Cu coating (Fig. 8a-1 and b-1). SLM observation shows remarkably inhibited adhesion of *Phaeodactylum tricornutum* and *Chlorella* on the copper-containing polyimide coatings. More Cu in the coatings results in less recruited algae (Fig. 8a and b). Moreover, it is observed that the PI-Cu coatings have 50–95% extinguishing efficiency against *Phaeodactylum tricornutum* and *Chlorella*. This is attributed presumably to continuous release of copper ions from the Cu-encapsulated coatings. The coating with the addition of 20 wt %Cu performs the best among the samples in terms of removal of the bacteria and the algae, suggesting possible synergistic effect of the distinct composite structure and release of copper.

4. Conclusions

Polyimide-copper coatings have been fabricated by liquid flame spray and the coatings have typical capsule structure with nano copper particles being enwrapped by polyimide shell. The polyimide splat exhibits micron-sized hollow structure with a tiny hole on its top surface, offering the splats the capability to release copper in a controllable manner. These structural characteristics facilitate constrained release of copper for antifouling functions and yet provide excellent anti-corrosion performances. The Cu-containing polyimide

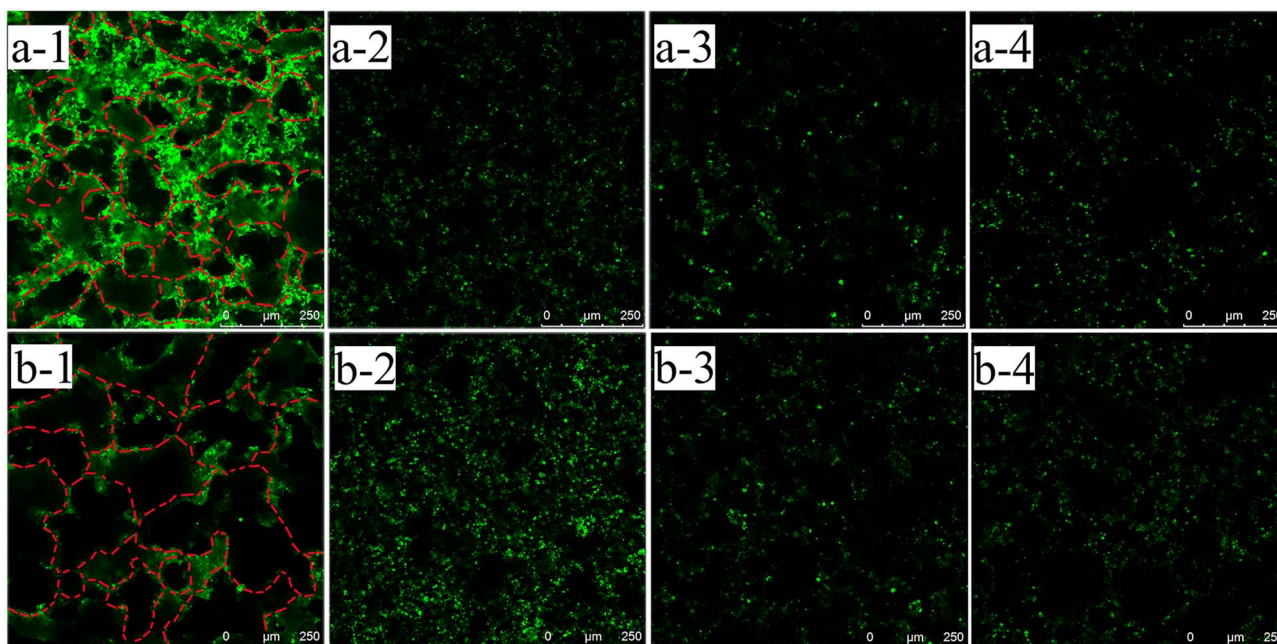


Fig. 8. Antifouling properties of the coatings, a: SLCM images showing colonization of *Phaeodactylum tricornutum* on the coatings after 7 days incubation, and b: SLCM images showing colonization of *Chlorella* on the coatings after 7 days incubation. (– 1: the pure polyimide coating, – 2: the polyimide-10 wt%Cu coating, – 3: the polyimide-20 wt%Cu coating, – 4: the polyimide-30 wt%Cu coating). The scale bar is 250 μm .

coatings show remarkable capability of resisting adhesion and colonization of *Bacillus* sp. bacteria and algae *Phaeodactylum tricornutum* and *Chlorella*. The newly constructed polyimide-Cu coatings show encouraging promises as anti-corrosion/fouling layers for marine structures. The thermal spray processing route might open a new window for making organic-inorganic composites or their coatings with capsule structure.

Acknowledgements

This work was supported by National Natural Science Foundation of China (grant # 31500772 and 41476064), Key Research and Development Program of Zhejiang Province (grant # 2017C01003), Project of Scientific Innovation Team of Ningbo (grant # 2015B11050), and China Postdoctoral Science Foundation (grant # 2014M561800 and 2016T90554).

References

- [1] J.A. Callow, M.E. Callow, Trends in the development of environmentally friendly fouling-resistant marine coatings, *Nat. Commun.* 2 (2011) 244.
- [2] M.E. Callow, J.A. Callow, Marine biofouling: a sticky problem, *Biologist* 49 (2002) 1–5.
- [3] I. Fritridge, T. Dempster, J. Guenther, R. de Nys, The impact and control of biofouling in marine aquaculture: a review, *Biofouling* 28 (2012) 649–669.
- [4] M. Thouvenin, J.J. Peron, C. Charette, P. Guerin, J.Y. Langlois, K. Vallee-Rehel, A study of the biocide release from antifouling paints, *Prog. Org. Coat.* 44 (2002) 75–83.
- [5] M.Y. Diego, K. Søren, D.J. Kim, Antifouling technology-past, present and future steps towards efficient and environmentally friendly antifouling coatings: review, *Prog. Org. Coat.* 50 (2004) 75–104.
- [6] S. Dobretsov, H.U. Dahms, P.I.Y. Qian, Inhibition of biofouling by marine microorganisms and their metabolites, *Biofouling* 22 (2006) 43–54.
- [7] M. Lejars, A. Margaillan, C. Bressy, Fouling release coatings: a nontoxic alternative to biocidal antifouling coatings, *Chem. Rev.* 112 (2012) 4347–4390.
- [8] S.M. Olsen, L.T. Pedersen, M.H. Laursen, S. Kiil, K. Dam-Johansen, Enzyme-based antifouling coatings: a review, *Biofouling* 23 (2007) 369–383.
- [9] J.L. Dalsin, P.B. Messersmith, Bioinspired polyimidederived antifouling polymers, *Mater. Today* 8 (2005) 38–46.
- [10] S. Krishnan, C.J. Weinman, C.K. Ober, Advances in polymers for anti-biofouling surfaces, *J. Mater. Chem.* 18 (2008) 3405–3413.
- [11] M.J. Vucko, P.C. King, A.J. Poole, C. Carl, M.Z. Jahedi, R. de Nys, Cold spray metal embedment: an innovative antifouling technology, *Biofouling* 28 (2012) 239–248.
- [12] Y. Liu, P. Guo, X.Y. He, L. Li, A.Y. Wang, H. Li, Developing transparent copper-doped diamond-like carbon films for marine antifouling applications, *Diam. Relat. Mater.* 69 (2016) 144–151.
- [13] T. Geiger, P. Delavy, R. Hany, J. Schleuniger, M. Zinn, Encapsulated zosteric acid embedded in poly [3-hydroxyalkanoate] coatings-protection against biofouling, *Polym. Bull.* 52 (2004) 65–72.
- [14] L. Nordstierna, A.A. Abdalla, M. Masuda, G. Skarnemark, M. Nydén, Molecular release from painted surfaces: free and encapsulated biocides, *Prog. Org. Coat.* 69 (2010) 45–48.
- [15] M.S. Selim, S.A. El-Safty, M.A. El-Sockary, A.I. Hashem, O.M. Abo Elenien, A.M. EL-Saeed, N.A. Fathallah, Smart photo-induced silicone/TiO₂ nanocomposites with dominant [110] exposed surfaces for self-cleaning foul-release coatings of ship hulls, *Mater. Des.* 101 (2016) 218–225.
- [16] A.V. Bers, M. Wahl, The influence of natural surface microtopographies on fouling, *Biofouling* 20 (2004) 43–51.
- [17] R. Zarzuela, M. Carbú, M.L.A. Gil, J.M. Cantoral, M.J. Mosquera, CuO/SiO₂ nanocomposites: a multifunctional coating for application on building stone, *Mater. Des.* 114 (2017) 364–372.
- [18] X. Wei, Z. Yang, Y. Wang, S.L. Tay, W. Gao, Polymer antimicrobial coatings with embedded fine Cu and Cu salt particles, *Appl. Microbiol. Biotechnol.* 98 (2014) 6265–6274.
- [19] S. Jiang, T. Sreethawong, S.S.C. Lee, M.B.J. Low, K.Y. Win, A.M. Brzozowska, S.L.-M. Teo, G.J. Vancso, D. Janczewski, M.-Y. Han, Fabrication of copper nanowire films and their incorporation into polymer matrices for antibacterial and marine antifouling applications, *Adv. Mater. Interfaces* 1400483 (2015) 1–8.
- [20] K.C. Anyaogu, A.V. Fedorov, D.C. Neckers, Synthesis, characterization, and antifouling potential of functionalized copper nanoparticles, *Langmuir* 24 (2008) 4340–4346.
- [21] A. Kerr, M.J. Smith, M.J. Cowling, T. Hodgkiess, The biofouling resistant properties of six transparent polymers with and without pre-treatment by two antimicrobial solutions, *Mater. Des.* 22 (2001) 383–392.
- [22] K. Vanherck, G. Koeckelberghs, I.F.J. Vankelecom, Crosslinking polyimides for membrane applications: a review, *Prog. Polym. Sci.* 38 (2013) 874–896.
- [23] Z. Chen, S. Liu, S. Yan, X. Shu, Y. Yuan, H. Huang, J. Zhao, Overall improvement in dielectric and mechanical properties of porous graphene fluoroxide/polyimide nanocomposite films via bubble-stretching approach, *Mater. Des.* 117 (2017) 150–156.
- [24] J. Tikkanen, K.A. Gross, C.C. Berndt, V. Polyimidetkänen, J. Keskinen, S. Raghu, M. Rajala, J. Karthikeyan, Characteristics of the liquid flame spray process, *Surf. Coat. Technol.* 90 (1997) 210–216.
- [25] J. Tharajak, T. Palathai, N. Sombatsompop, Recommendations for h-BN loading and service temperature to achieve low friction coefficient and wear rate for thermal-sprayed PEEK coatings, *Surf. Coat. Technol.* 321 (2017) 477–483.
- [26] C.J. Weng, J.Y. Huang, K.Y. Huang, Y.S. Jhuo, M.H. Tsai, J.M. Yeh, Advanced anticorrosive coatings prepared from electroactive polyimide-TiO₂ hybrid nanocomposite materials, *Electrochim. Acta* 55 (2010) 8430–8438.
- [27] X. Wang, Y. Liu, Y.F. Gong, X.K. Suo, H. Li, Liquid flame spray fabrication of polyimide-copper coatings for antifouling applications, *Mater. Lett.* 190 (2017) 217–220.
- [28] M. Pasandideh-Fard, V. Pershin, S. Chandra, J. Mostaghimi, Splat shapes in a thermal spray coating process: simulations and experiments, *J. Therm. Spray*

- Technol. 11 (2002) 206–217.
- [29] Y. Li, X. Pei, B. Shen, W. Zhai, L. Zhang, W. Zheng, Polyimide/graphene composite foam sheets with ultrahigh thermostability for electromagnetic interference shielding, *RSC Adv.* 5 (2015) 24342–24351.
- [30] P. Fauchais, A. Vardelle, A. Denoirjean, Reactive thermal plasmas: ultrafine particle synthesis and coating deposition, *Surf. Coat. Technol.* 97 (1997) 66–78.
- [31] H. Liu, J. Huang, Reactive thermal spraying of TiC-Fe composite coating by using asphalt as carbonaceous precursor, *J. Mater. Sci.* 40 (2005) 4149–4151.
- [32] Y. Zhu, Y. Ma, Q. Yu, J.X. Wei, J. Hu, Preparation of pH-sensitive core-shell organic corrosion inhibitor and its release behavior in simulated concrete pore solutions, *Mater. Des.* 119 (2017) 254–262.
- [33] P. Subalakshmi, M. Ganesan, A. Sivashanmugam, Synthesis of 3D architecture CuO micro balls and nano hexagons and its electrochemical capacitive behavior, *Mater. Des.* 119 (2017) 104–112.
- [34] B. Bhushan, Y.C. Jung, K. Koch, Micro-, nano-and hierarchical structures for superhydrophobicity, self-cleaning and low adhesion, *Philos. Trans. R. Soc. London, Ser. A* 367 (2009) 1631–1672.
- [35] J.E. George, V.R.M. Rodrigues, D. Mathur, C. Santhosh, Sajan D. George, Self-cleaning superhydrophobic surfaces with underwater superaerophobicity, *Mater. Des.* 100 (2016) 8–18.
- [36] A. Marmur, Super-hydrophobicity fundamentals: implications to biofouling prevention, *Biofouling* 22 (2006) 107–115.
- [37] R.B. Thurman, C.P. Gerba, G. Bitton, The molecular mechanisms of copper and silver ion disinfection of bacteria and viruses, *Crit. Rev. Environ. Sci. Technol.* 18 (1989) 295–315.
- [38] P. Setlow, Mechanisms for the prevention of damage to DNA in spores of bacillus species, *Annu. Rev. Microbiol.* 49 (1995) 29–54.
- [39] H.H.P. Fang, L.C. Xu, K.Y. Chan, Effects of toxic metals and chemicals on biofilm and biocorrosion, *Water Res.* 36 (2002) 4709–4716.